

Supplemental material

Spencer et al., <https://doi.org/10.1084/jem.20190344>

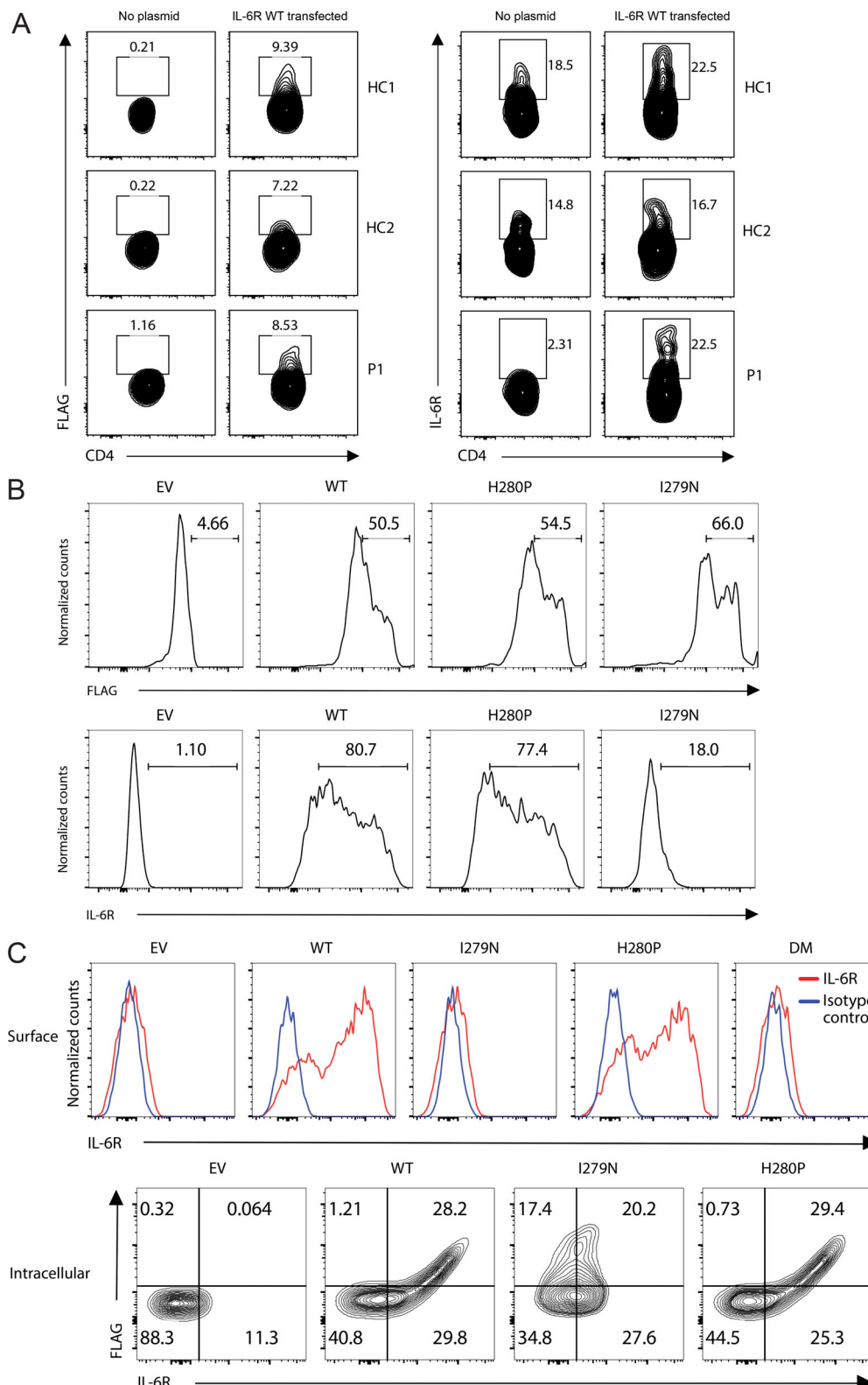


Figure S1. Assessment of ectopic IL6R expression. **(A)** PBMCs from healthy controls (HC) and P1 were isolated from Ficoll gradient and transfected with WT IL-6R cDNA cloned in the pcDNA3.1⁺/C-(K)-DYK plasmid using T cell nucleofection. After 24 h, the PBMCs were intracellularly stained with anti-CD4, anti-FLAG, and anti-IL-6R antibodies and analyzed by flow cytometry. **(B)** HEK293 cells were transfected with empty vector (EV), WT, H280P, and I279N mutants cloned in the pcDNA3.1⁺/C-(K)-DYK plasmid. After 24 h, the proteins and transfection efficiencies were measured by flow cytometry using anti-FLAG and IL-6R antibody (UV4). Similar results were observed when stained with the IL-6R clone M5 (not depicted). **(C)** Human healthy PBMCs were transfected with empty vector (EV), WT, I279N, H280P, and I279N/H280P (DM) mutants using T cell nucleofection. After 24 h, the proteins and transfection efficiencies were measured by flow cytometry using anti-FLAG and IL-6R antibody (UV4). Top: Surface staining (red, IL-6R; blue, isotype control). Bottom: Intracellular staining.

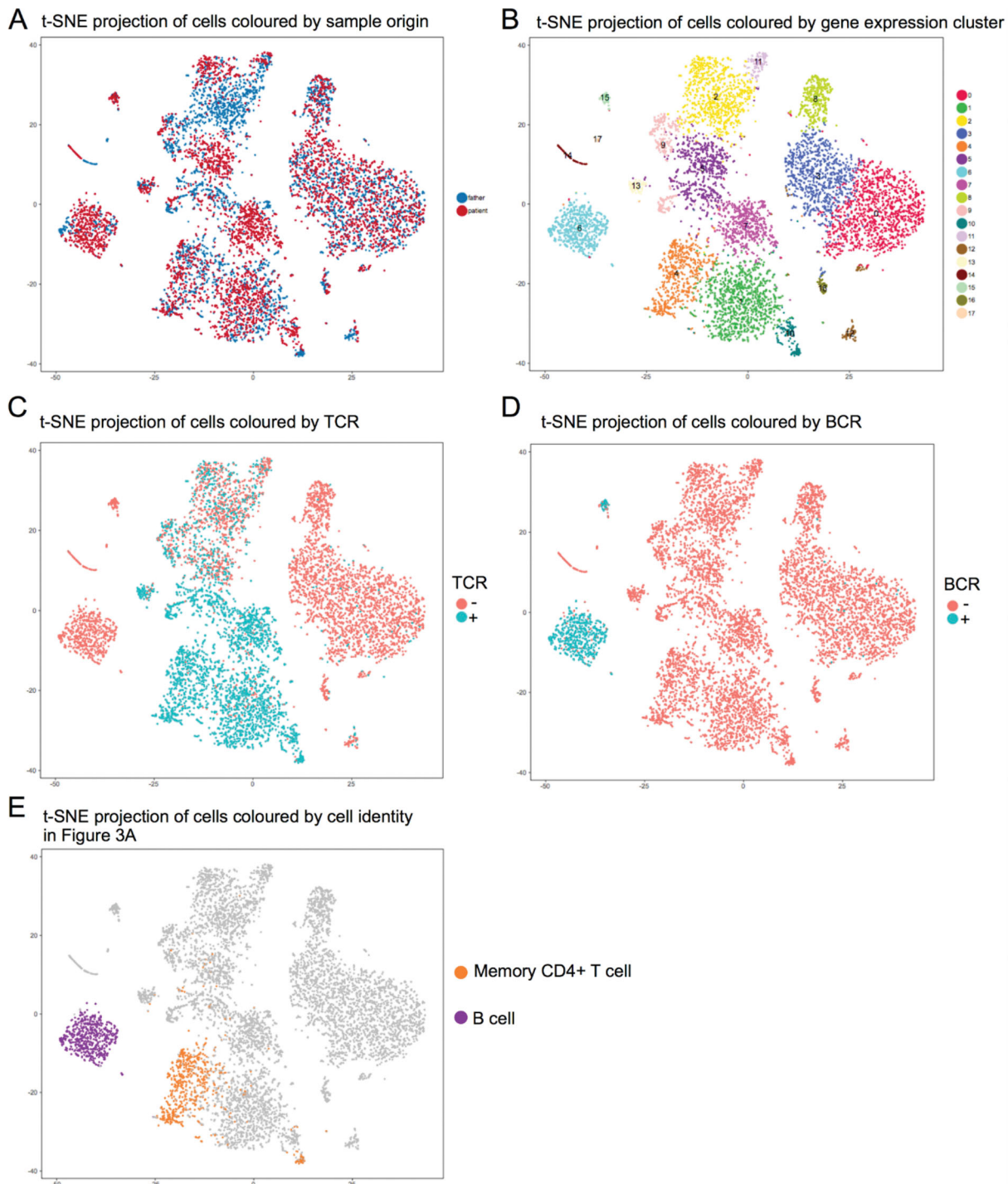


Figure S2. tSNE projections of PBMCs from the IL-6R-null patient (P1) and her father (HP1). **(A–D)** Clusters of single cells are identified using a shared-nearest-neighbor graph (Xu and Su, 2015). Each cell is assigned a cluster. The clustering groups together cells that have similar expression profiles. tSNE plots are color coded by sample (A), gene expression cluster membership (B), TCR presence (C), and B cell receptor (BCR; D). **(E)** Memory CD4⁺ T and B cells were identified by gene expression or TCR or BCR presence and assigned for the differentiation analysis displayed in Fig. 3 A.

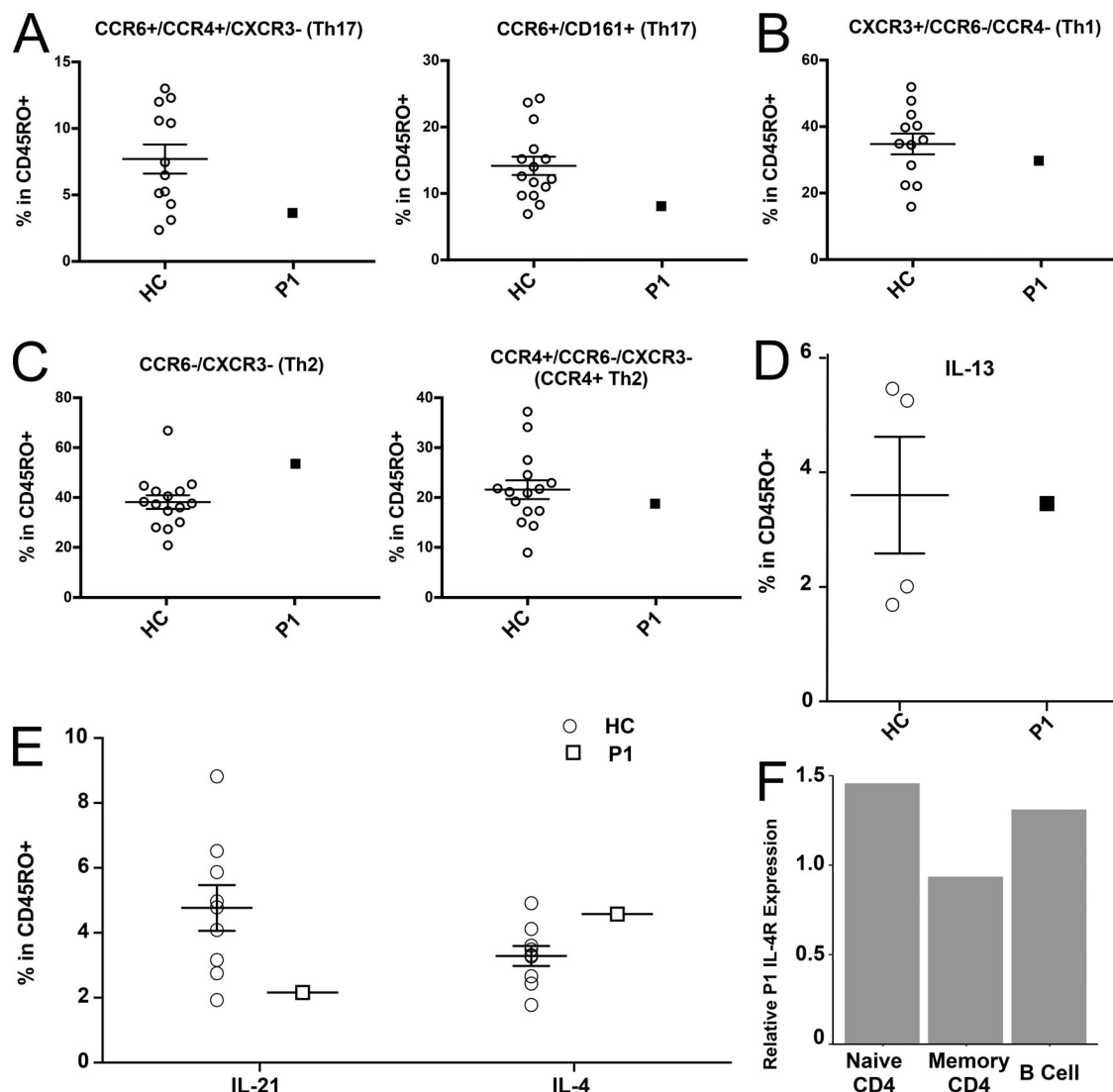


Figure S3. Phenotype assessment of P1. **(A–C)** FACS assessment of the indicated surface markers used to identify memory CD4⁺ Th17 (A), Th1 (B), and Th2 (C) T cells. **(D and E)** FACS analysis of the intracellular cytokine staining of healthy control (HC) and P1 PBMCs after PMA and ionomycin stimulation for IL-21 and IL-4 (D) and IL-13 (E). **(F)** Relative average expression of *IL4R* in the patient with respect to the father, within naive CD4⁺ and memory CD4⁺ T cell and B cell populations. For each cluster, mean *IL4R* expression was calculated for patient and father cells. These values were divided to obtain the fold-change of average expression between the two samples. Error bars represent SEM.

Table S1. Comparative analysis of clinical features of patients with *IL6R* mutations and other patient cohorts with defined gene defects presenting with elevated IgE

| | <i>IL6R</i> | <i>IL6ST</i> | <i>STAT3</i> | <i>ZNF341</i> | <i>DOCK8</i> | <i>CARD11</i> | <i>PGM3</i> | <i>ERBIN</i> |
|-------------------------------|----------------|----------------|-----------------|-----------------|----------------|----------------|-----------------|----------------|
| <i>n</i> | 2 | 2 | 140 | 19 | 64 | 12 | 29 | 3 |
| Inheritance | AR | AR | AR | AR | AR | AD | AR | AD |
| IgE | ↑ ^a | ↑ ^a | ↑↑ ^a | ↑↑ ^a | ↑ ^a | ↑ ^a | ↑↑ ^a | ↑ ^a |
| Eosinophilia | + | + | + | +/- | + | + | + | + |
| Eczema | ++ | + | + | + | ++ | ++ | + | + |
| Infections | | | | | | | | |
| Abscess | ++ | -/+ | ++ | + | + | + | ++ | - |
| Pneumonia | ++ | ++ | +++ | + | + | ++ | ++ | ++ |
| Sinusitis/otitis | + | + | + | + | ++ | + | + | + |
| Candidiasis | - | - | ++ | ++ | + | + | + | - |
| Viral infections | - | - | + | - | +++ | + | ++ | - |
| Musculoskeletal abnormalities | - | ++ | ++ | + | + | +/- | - | - |
| IgE hypersensitivity | - | + | + | + | +++ | +++ | +++ | + |
| Autoimmunity | - | - | + | - | ++ | + | ++ | - |
| CNS abnormalities | - | ++ | + | + | ++ | - | ++ | - |
| Neoplasia | - | - | + | +/- | ++ | - | + | - |
| Immunological features | | | | | | | | |
| Immunoglobulins | Normal/low | Normal | Normal | Normal/high IgG | Normal/low | Normal/low | Normal | Normal |
| Lymphopenia | - | - | - | +/- | +/- | - | + | - |
| Th17 cells | Normal/low | Normal/low | Low | Low | Low | Normal | Normal | Normal |
| CD19 ⁺ B cells | Normal | Normal/low | Normal/low | Normal | Normal/low | Normal/low | Normal/low | Normal |
| Switched-memory B cells | Low | Normal/low | Low | Low | Low | Normal/low | Normal/low | Normal |

Recently a comprehensive table comparing phenotypes with elevated IgE was also presented in [Shahin et al., 2019](#). AD, autosomal dominant; AR, autosomal recessive; CNS, central nervous system.

^a↑↑ refers to IgE levels >5,000 IU/ml; ↑ refers to IgE levels 1,000–5,000 IU/ml.

Table S2. Filtered homozygous C1 variants identified in P1 and filtered homozygous variants in P2

| Gene | Gene description | Coding effect | Genomic annotation (GRCh37) | cDNA annotation | Protein annotation | gnomAD AF | CADD score |
|----------|---|---------------|-----------------------------|-------------------------------|------------------------------------|------------|------------|
| P1 | | | | | | | |
| MAP7D1 | MAP7 domain containing 1 | Missense | chr1:g.36641812A>G | ENST00000316156.4: c.863A>G | ENSP00000320228.4: p.Gln288Arg | 0.00003237 | 17.7 |
| PIK3R3 | Phosphoinositide-3-kinase regulatory subunit 3 | Stop gain | chr1:g.46642005G>A | ENST00000540385.1: c.139C>T | ENSP00000439913.1: p.Arg47* | 0.00001619 | 31.0 |
| CCDC18 | Coiled-coil domain containing 18 | Stop gain | chr1:g.93711681G>T | ENST00000343253.7: c.2998G>T | ENSP00000343377.7: p.Glu1000* | 0.00001247 | 50.0 |
| IL6R | Interleukin-6 receptor | Frameshift | chr1:g.154407084del | ENST00000368485.3: c.548del | ENSP00000357470.3: p.Gly183Glufs*7 | 0 | NA |
| NES | Nestin | Missense | chr1:g.156639266C>T | ENST00000368223.3: c.4714G>A | ENSP00000357206.3: p.Glu1572Lys | 0 | 21.1 |
| PLXNA2 | Plexin A2 | Missense | chr1:g.208218435G>A | ENST00000367033.3: c.3616C>T | ENSP00000356000.3: p.Leu1206Phe | 0.00004329 | 23.6 |
| KCTD3 | Potassium channel tetramerization domain containing 3 | Missense | chr1:g.215792524C>T | ENST00000259154.4: c.177C>T | ENSP00000259154.2: p.Leu593Phe | 0.00000813 | 24.6 |
| P2 | | | | | | | |
| MAB21L3 | Mab21-like-3 | Splice donor | chr1:g.116666979G>T | ENST00000369500.3: c.481+1G>T | ENST00000369500.3: c.481+1G>T | 0.000125 | 33.0 |
| CYP26A1 | Cytochrome p450 | Missense | chr10:g.94836739G>A | ENST00000224356.4: c.1172G>A | ENST00000224356.4: c.1172G>A | 0.000398 | 31.0 |
| TECTA | Tectorin alpha | Missense | chr11:g.121016276C>T | ENST00000392793.1: c.3556C>T | ENST00000392793.1: c.3556C>T | 0.000874 | 28.3 |
| SLC25A24 | Solute carrier family 25 | Splice donor | chr1:g.108742577C>A | ENST00000565488.1: c.183+1G>T | ENST00000565488.1: c.183+1G>T | 0 | 28.1 |
| PEAR1 | Platelet endothelial aggregation receptor | Missense | chr1:g.156877958A>G | ENST00000338302.3: c.941A>G | ENST00000338302.3: c.941A>G | 0.0000258 | 27.5 |
| TRIM69 | Tripartite motif containing protein | Missense | chr15:g.45050880T>C | ENST00000559390.1: c.641T>C | ENST00000559390.1: c.641T>C | 0.00000406 | 27.2 |
| ARHGEF12 | Rho guanine nucleotide exchange factor 12 | Missense | chr11:g.120328462G>A | ENST00000397843.2: c.2222G>A | ENST00000397843.2: c.2222G>A | 0.000252 | 27.0 |
| IL6R | Interleukin 6 receptor alpha | Missense | chr1:g.154408473T>A | ENST00000368485.3: c.836T>A | ENST00000368485.3: c.836T>A | 0 | 24.8 |
| DIXDC1 | DIX-domain containing 1 | Missense | chr11:g.111845662A>G | ENST00000440460.2: c.611A>G | ENST00000440460.2: c.611A>G | 0.000399 | 24.3 |
| SPTA1 | Spectrin alpha | Missense | chr1:g.158585147A>G | ENST00000368147.4: c.6647T>C | ENST00000368147.4: c.6647T>C | 0.0000122 | 23.8 |
| DLG5 | Discs large 5 | Missense | chr10:g.79577595C>T | ENST00000372391.2: c.3724G>A | ENST00000372391.2: c.3724G>A | 0.0000196 | 23.8 |
| STARD9 | Start domain containing protein 9 | Missense | chr15:g.43009197C>T | ENST00000290607.7: c.13445C>T | ENST00000290607.7: c.13445C>T | 0.000859 | 23.2 |
| SORBS1 | SORBIN and SH3 domains containing protein 1 | Missense | chr10:g.97096822G>C | ENST00000371247.2: c.3095C>G | ENST00000371247.2: c.3095C>G | 0.000834 | 23.1 |
| OR6K3 | Olfactory receptor family 6 subfamily K member 3 | Missense | chr1:g.158687688T>A | ENST00000368145.1: c.218A>T | ENST00000368145.1: c.218A>T | 0 | 22.5 |
| ALG8 | Alpha-1,3-glucosyltransferase | Missense | chr11:g.77812075C>T | ENST00000299626.5: c.1516G>A | ENST00000299626.5: c.1516G>A | 0.000427 | 20.9 |
| WDR47 | WD repeat domain 47 | Missense | chr1:g.109538319T>C | ENST00000400794.3: c.1598A>G | ENST00000400794.3: c.1598A>G | 0.0000487 | 20.4 |
| SV2A | Synaptic vesicle glycoprotein 2A | Missense | chr1:g.149878301T>G | ENST00000369146.3: c.1786A>C | ENST00000369146.3: c.1786A>C | 0.0000651 | 19.0 |

Table S2. Filtered homozygous C1 variants identified in P1 and filtered homozygous variants in P2 (Continued)

| Gene | Gene description | Coding effect | Genomic annotation (GRCh37) | cDNA annotation | Protein annotation | gnomAD AF | CADD score |
|---------|----------------------------------|-------------------|-----------------------------|---------------------------------|---------------------------------|------------|------------|
| ASTN2 | Astrotactin 2 | Missense | chr9:g.120177057C>T | ENST00000361209.2: c.160G>A | ENST00000361209.2: c.160G>A | 0 | 18.8 |
| IFT81 | Intraflagellar transport 81 | Missense | chr12:g.110566928A>G | ENST00000242591.5: c.422A>G | ENST00000242591.5: c.422A>G | 0.000359 | 18.3 |
| SOX4 | SRY-Box4 | In-frame deletion | chr6:g.21595443_21595445del | ENST00000244745.1: c.678_680del | ENST00000244745.1: c.678_680del | 0.00006620 | 16.7 |
| EMILIN1 | Elastin microfibril interfacer 1 | Missense | chr2:g.27306843G>A | ENST00000380320.4: c.2404G>A | ENST00000380320.4: c.2404G>A | 0 | 15.9 |
| IL6R | Interleukin 6 receptor alpha | Missense | chr1:g.154408476A>C | ENST00000368485.3: c.839A>C | ENST00000368485.3: c.839A>C | 0 | 10.5 |

References

- Shahin, T., D. Aschenbrenner, D. Cagdas, S.K. Bal, C.D. Conde, W. Garncarz, D. Medgyesi, T. Schwerd, B. Karaatmaca, P.G. Cetinkaya, et al. 2019. Selective loss of function variants in *IL6ST* cause Hyper-IgE syndrome with distinct impairments of T-cell phenotype and function. *Haematologica*. 104:609–621. <https://doi.org/10.3324/haematol.2018.194233>
- Xu, C., and Z. Su. 2015. Identification of cell types from single-cell transcriptomes using a novel clustering method. *Bioinformatics*. 31:1974–1980. <https://doi.org/10.1093/bioinformatics/btv088>